A model of C_4 photosynthetic acclimation based on least-cost optimality theory suitable for Earth System Model incorporation

Helen G. Scott[1], **Nicholas G. Smith**[1]

[1]Texas Tech University, 2901 Main St., Lubbock, TX 79409

Key Points:

- A parameter-sparse model of C_4 photosynthetic acclimation to changes in environmental conditions based on photosynthetic least cost theory is presented.
- The model suggests that including acclimation will improve simulations of C_4 carbon assimilation as well as their water use and nutrient use efficiencies under present day and projected future conditions.
- In simulated competition experiments with a similar C_3 model, it is found that C_4 photosynthesis becomes less advantageous under increased temperature and carbon dioxide conditions.

Corresponding author: Helen G. Scott, `helengracescott@gmail.com`

Abstract

Empirical studies have shown that plant photosynthetic responses to environmental change can vary over time due to acclimation, but acclimation responses are often not included in Earth System Models. Photosynthetic least cost theory can be used to develop models of photosynthetic acclimation that are simple and testable. The theory is based on the idea that, optimally, plants will acclimate to maintain the fastest rate of photosynthesis at the lowest water and nutrient use. Formulations of this theory have been developed for C_3 plants, but not C_4 plants, which account for over 20% global photosynthesis and are over-represented among widely grown crops. Here, we use photosynthetic least cost theory to derive a model for C_4 photosynthetic acclimation to above-ground abiotic conditions. We then compare our model's responses to a similar model of C_3 photosynthetic acclimation and find that C_4 photosynthesis has the highest simulated advantage over C_3 photosynthesis in hot, dry, and low CO_2 environments. We find that this advantage predicts C_4 abundance globally, but that the shallower CO_2 response of C_4 as compared to C_3 photosynthesis will reduce C_4 plant competitiveness under future conditions, despite higher temperatures. We also show that an acclimated model predicts similar or faster rates of C_4 under all conditions than a model that does not consider acclimation, suggesting that Earth System Models (ESMs) are underestimating future C_4 carbon uptake by not including acclimation. Our model is designed for easy incorporation into such ESMs.

Plain Language Summary

Plants change their rate of photosynthesis in response to their environment. Their photosynthetic rates can change minute to minute based on the quick changes in their environment, but they can also change over much longer time scales as the plants become accustomed to a new environmental condition. This long term regulation of photosynthesis is termed acclimation. When we predict how plants will behave into the future we must take acclimation into account so that we can more accurately predict the future carbon, water, and nutrient cycles. Previous studies have developed mathematical models of photosynthetic acclimation for some, but not all, plants. One understudied group of plants that lacked an acclimation model were the C_4 species, a subtype of plants often found in deserts and other arid environments, but one that also include important agricultural crops such as maize. In this study we develop a theoretical model of photosynthetic acclimation for C_4 species, and show that the model yields expected results based on where C_4 plants currently grow. Our model can improve predictions of carbon, water, and nutrient cycling in larger Earth System Models.

1 Introduction

Current Earth System Models (ESMs) are highly sensitive to the representation of photosynthetic processes and their response to environmental conditions (Booth et al., 2012). These models commonly predict photosynthetic process rates based on instantaneous responses (i.e., seconds to minutes) (Smith & Dukes, 2013). However, decades of empirical studies have shown that plants adjust their responses when subjected to longer-term (days to weeks) changes in environmental conditions, due to acclimation (Boardman, 1977; Berry & Bjorkman, 1980; Bazzaz, 1990; Dusenge et al., 2019; Yamori et al., 2014; Smith & Dukes, 2013; Way & Yamori, 2014). Previous studies have shown that including C_3 photosynthetic acclimation alters biophysical and biogeochemical feedback in ESMs (Smith et al., 2017, 2016; Lombardozzi et al., 2015; Mercado et al., 2018; King et al., 2006; Kattge & Knorr, 2007; Thornton et al., 2007a; Friend, 2010; Zaehle & Friend, 2010). However, there is no acclimation model for plants that use the C_4 photosynthetic pathway. Photosynthetic acclimation has been observed for C_4 species (Dwyer et al., 2007; Smith & Dukes, 2017; R. F. Sage, 1999; Bellasio & Griffiths, 2014; Yamori et al., 2014), and

may occur through changes in both stomatal (Maherali et al., 2002; Bellasio & Griffiths, 2014) and biochemical (Smith & Dukes, 2017; R. Sage & Kubien, 2007) processes. However, it is essential to note that these acclimation responses may differ from those observed in C_3 species (Maherali et al., 2002; Yamori et al., 2014). For instance, the mesophyll cells of C_4 leaves contain phosphoenolpyruvate carboxylase (PEPc), which captures incoming CO_2 and shuttles carbon to ribulose-1,5-bisphosphate carboxylase/oxygenase (RuBisCO) in specialized bundle sheath cells (Kanai & Edwards, 1999). The high concentration of carbon shuttled to the bundle sheath cells increases the relative amount of carboxylation versus oxygenation that RuBisCO performs (Kanai & Edwards, 1999). Because of this specialized anatomy, C_4 species operate at lower stomatal conductance rates than C_3 species and show a reduced sensitivity of photosynthetic processes to CO_2, temperature, and vapor pressure deficit (R. F. Sage, 1999). High CO_2 concentrations in the bundle sheath and the Kranz anatomy partially explain dampened acclimation responses in C_4 species (Yamori et al., 2014; Maherali et al., 2002; R. F. Sage & McKown, 2006). However, there are not many experimental comparisons available in the literature.

In complement to empirical studies, theoretical models of photosynthetic functioning can help elucidate the mechanisms underlying environmental responses (Collatz et al., 1992; Ehleringer et al., 1997; Wang et al., 2017; Zhou et al., 2018; G. D. Farquhar et al., 1980; Collatz et al., 1991). Classic work has used these models to compare simulated photosynthetic rates of C_3 and C_4 species under varying environmental conditions as a way of explaining geographic patterns in the abundance of species utilizing different photosynthetic pathways (Ehleringer et al., 1997). Other studies have used acclimation models to predict historical ranges of C_4 plants at geologic timescales (Zhou et al., 2018). These studies have confirmed C_4 advantages in warm, arid, high light, and low CO_2 environments. However, these studies have either omitted acclimation (Ehleringer et al., 1997) or only included simplified empirical representations (Zhou et al., 2018). The recent development of theoretical models for C_3 photosynthetic acclimation (Wang et al., 2017) presents the opportunity to perform similar theoretical comparisons between C_3 and C_4 species while accounting for acclimation with the complimentary development of a theoretical model for C_4 photosynthesis.

Here, we develop a novel theoretical model of C_4 photosynthetic acclimation to aboveground environmental conditions. The model is based on the least-cost theory of photosynthesis (Wright et al., 2003), extending the original theory based on C_3 species to C_4 species. At its core, the least-cost theory suggests that, optimally, plants should acclimate under average environmental conditions such that they perform the fastest rates of photosynthesis at the lowest resource cost. The primary resource costs are water and nutrients to support transpiration and photosynthetic biochemistry, respectively. We develop the model using a similar approach to Wang et al. (2017) and use it to predict acclimated values for intracellular CO_2, photosynthetic biochemistry, and photosynthesis of C_4 leaves under varying environmental conditions.

We use the theoretical model to compare responses to environmental conditions in leaves under acclimated and non-acclimated conditions to explore potential impacts the model might have on carbon uptake if included in an ESM. We also replicate classical theoretical competition experiments (Ehleringer et al., 1997) to explore the conditions under which C_4 species have greater carbon assimilation rates than C_3 species.

2 Methods

We developed this theoretical model of C_4 photosynthetic acclimation by combining the coordination theory of photosynthetic biochemistry (Maire et al., 2012; Chen et al., 1993) and the least-cost hypothesis of stomatal conductance (Prentice et al., 2014; Wright et al., 2003). The primary assumption is that, optimally, acclimated plants will maintain the highest carbon gain at the lowest water and nutrient use. Figure 1 shows a schematic representation of the model. The least-cost hypothesis predicts the optimal ratio of in-

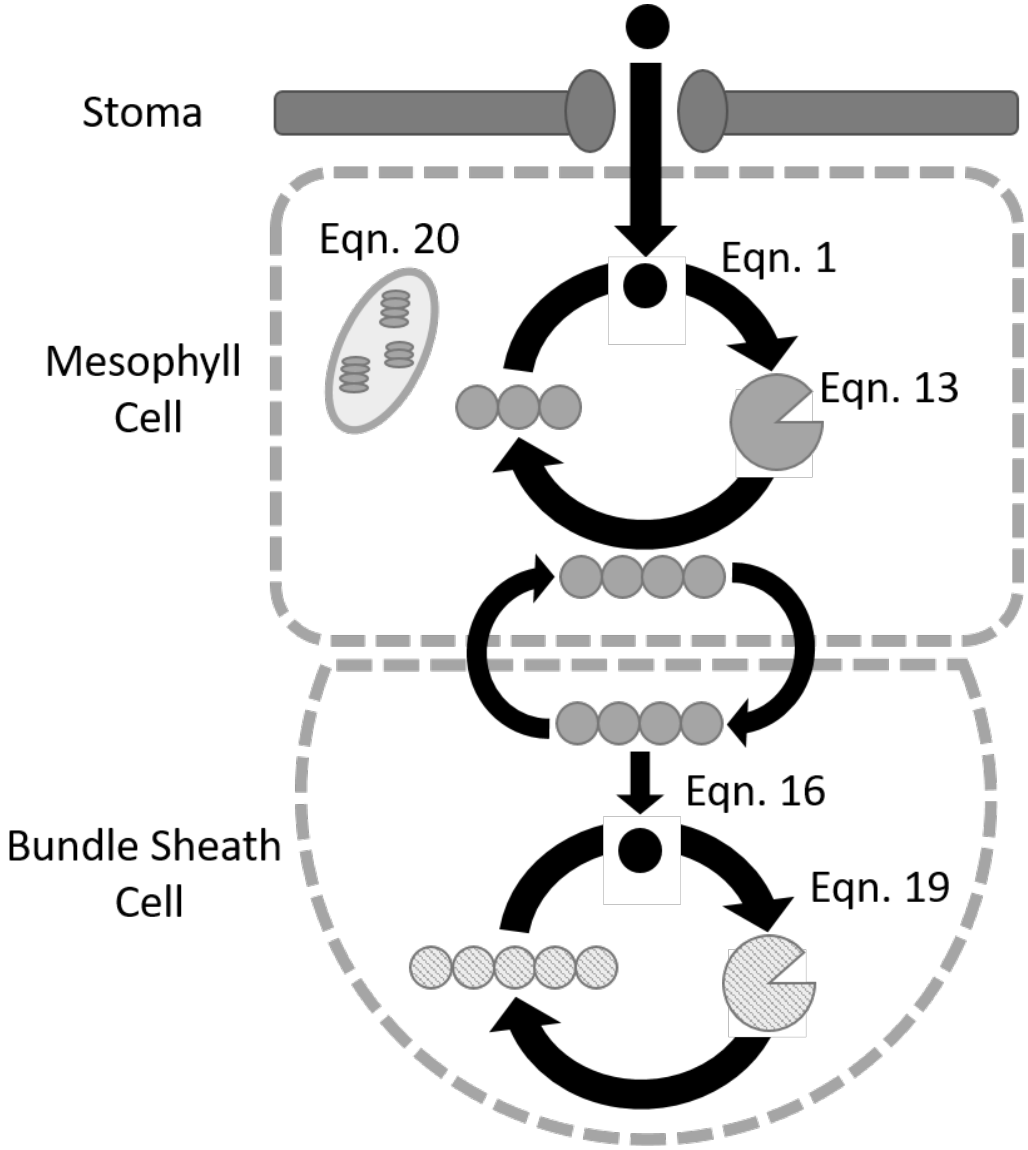

Figure 1: Schematic representation of the main features of the acclimated C_4 model. CO_2 diffuses into the mesophyll cell, where it is fixed into a C_4 acid by PEPc at the rate of V_{pmax}. The C_4 is concentrated in the bundle sheath at the rate of g_{bs}, where it is unpackaged, and fixed by RuBisCO at the rate of V_{cmax}. The rate of the electron transport chain (J_{max}) limits PEP and RuBP regeneration. Arrows indicate the path of molecule diffusion.

tercellular CO_2 (C_i) to atmospheric CO_2 (C_a), referred to here as χ_m. We then use χ_m to estimate the concentration of CO_2 in the mesophyll cell (C_m) and the bundle sheath cell (C_{bs}). These CO_2 concentrations, along with the growing season conditions of light available for photosynthesis (photosynthetically active radiation, or PAR) and temperature, serve as inputs to calculate the maximum rates of carboxylation by PEPc (V_{pmax}) and RuBisCO (V_{cmax}) as well as electron transport (J_{max}). First, we present a theoretical model to estimate χ_m, parameterized with a worldwide data set of isotope discrimination in C_4 plants. We then describe how we use the coordination theory to predict optimal J_{max}, V_{pmax}, and V_{cmax}.

2.1 Optimal C_m Calculation

We developed a modified version of the C_3 least-cost model from Prentice et al. (2014) for C_4 plants to calculate the partial pressure of CO_2 present in the mesophyll cells (C_m (Pa)). We calculate C_m as a fraction of atmospheric CO_2 (c_a (Pa)).

$$C_m = \chi_m c_a \tag{1}$$

χ_m is the ratio of atmospheric to mesophyll CO_2, we define it as:

$$\chi_m = \frac{\xi}{\xi + \sqrt{D}}, \text{ where } \xi = \sqrt{\frac{\beta K_p}{1.6\eta^*}} \tag{2}$$

where D is the vapor pressure deficit (Pa), K_p is the Michaelis-Menten constant for for PEPc (Pa), and η^* is the viscosity of water relative to its value at 25 °C ($\eta^* = \eta/\eta_{ref}$; unitless).
The value β (unitless) in equation 2 is the ratio (b/a) of dimensionless cost factors for maintaining carboxylation (b) to maintaining transpiration (a). We use a value of 166 for β, which was fit using a wold-wide data set of carbon isotope discrimination values for C_4 species (Cornwell et al., 2018). This β value is in contrast to the β value for C_3 plants, 240 (Wang et al., 2017).
Here, we assumed that the mesophyll conductance (the movement of CO_2 from the intercellular spaces to the mesophyll cell) was 1. As such, C_m was equal to the intercellular CO_2 (C_i).
For the full derivation of 2, see the supplemental information.

2.2 Coordination Hypothesis

The rate of C_4 photosynthetic assimilation (A) is the minimum value of possible photosynthetic rates limited by different factors (Von Caemmerer & Furbank, 1999; Von Caemmerer, 2000; Collatz et al., 1992). The three primary limiting rates for C_4 photosynthesis are: (1) electron transport rate-limited photosynthesis (A_L), limited by enzymes that use PAR to drive the electron transport chain that regenerates PEP and RuBisCO, (2) PEPc limited photosynthesis (A_P), limited by the rate of carboxylation by PEPc, and (3) RuBisCO limited photosynthesis (A_C), limited by the rate of RuBisCO carboxylation. The rate of photosynthesis (A) in C_4 plants can be represented as:

$$A = \min\{A_L, A_P, A_C\} \tag{3}$$

The coordination hypothesis states that under acclimated conditions, optimal leaf biochemistry will lead to equal rates of (A_L), (A_P), and (A_C) or

$$A_L = A_P = A_C \tag{4}$$

These three rates vary independently from one another based on above-ground environmental conditions, including PAR, temperature, CO_2, and vapor pressure deficit (VPD), allowing us to derive optimally acclimated biochemical rates under different acclimated conditions. To do this, we calculated A_L as in Smith et al. (2019):

$$A_L = \frac{\phi I m \omega^*}{8\theta} \tag{5}$$

where

$$m = \frac{C_i - \Gamma^*}{C_i + 2\Gamma^*} \tag{6}$$

and

$$\omega^* = 1 + \omega - \sqrt{(1+\omega)^2 - 4\theta\omega} \tag{7}$$

and

$$\omega = -(1-2\theta) + \sqrt{(1-\theta)\left(\frac{1}{\frac{4c}{m}(1-\theta\frac{4c}{m})} - 4\theta\right)} \tag{8}$$

where I is the incident photosynthetically active photon flux density (μmol m^{-2}s^{-1}), θ is the curvature of the PAR response curve, assumed to be 0.85 (unitless), and ϕ is the realized quantum yield of photosynthetic electron transport (mol mol^{-1}). Γ^* is the photorespiratory CO_2 compensation point (calculated below in equation 10). For the calculation of ω, we assumed the non-varying parameter c, defined as the derivative of A_L with respect to the maximum rate of electron transport (J_{max}), to be equivalent to the standard value for C_3 species, 0.053 (Smith et al., 2019). ϕ is itself dependent on temperature and was simulated as in Bernacchi et al. (Bernacchi et al., 2003):

$$\phi = -0.0805 + 0.022T - 0.00034T^2 \tag{9}$$

which corresponds to a ϕ value of 0.257 at 25 °C, as has been found for C_3 plants (Smith et al., 2019). There is evidence that the ϕ_{25} value may be significantly higher in C_4 species (Oberhuber & Edwards, 1993; Krall et al., 1991), though a single reference value is not widely used currently. The value used for the intercept term of equation 9 does not impact the predicted environmental responses. Γ^* varies with temperature according to:

$$\Gamma^* = \Gamma^*_{25} \exp\left[\frac{\Delta H_{a(g)}}{R}\left(\frac{1}{298.15} - \frac{1}{T}\right)\right] \tag{10}$$

where Γ^*_{25} is 2.6 Pa at sea level, determined by using the definition $\Gamma^*_{25} = \gamma^* O_m$, where γ^* is half the reciprocal of RuBisCO specificity, 0.000193 (Von Caemmerer, 2000). $\Delta H_{a(g)}$ is 37830 J mol^{-1}, T is the acclimated leaf temperature in Kelvin, and R is the ideal gas constant (Bernacchi et al., 2001).

A_P is typically defined using the standard Michaelis-Menten equation of enzyme kinetics:

$$A_P = \frac{V_{pmax} C_m}{K_p + C_m} \tag{11}$$

where V_{pmax} is the maximum rate of PEPc carboxylation (μ mol m^{-2} s^{-1}), K_p is the Michaelis-Menten constant for PEPc (Pa), and C_m is the concentration of CO_2 at the site of carboxylation, the mesophyll chloroplast (Pa). K_p is dependent on temperature in the following manner:

$$K_p = K_{p(25)} \exp\left[\Delta H_{a(p)} \frac{T - 298.15}{298.15RT}\right] \tag{12}$$

where $K_{p(25)}$ is equal to 60.5 μmol mol^{-1} and $\Delta H_{a(p)}$ is equal to 27.2 kJ mol^{-1} (Boyd et al., 2015). Using equation 5 and 11, we can solve for optimal V_{pmax} as:

$$V_{pmax} = \frac{\phi I m \omega^*}{8\theta} \frac{K_p + C_m}{C_m} \tag{13}$$

A_C can also be defined using the Michaelis-Menten equation:

$$A_C = \frac{V_{cmax}(C_{bs} - \Gamma^*)}{K_c(1 + O_{bs}/K_o) + C_{bs}} \tag{14}$$

K_c is the Michaelis-Menten coefficient of RuBisCO's carboxylation activity (Pa) and C_{bs} is the concentration of CO_2 at the carboxylation site, the bundle sheath cell (Pa). K_c responds to temperature as follows:

$$K_c = K_{c(25)} \exp\left[\Delta H_{a(c)} \frac{T - 298.15}{298.15RT}\right] \tag{15}$$

Where $K_{r(25)}$ is equal to 121 Pa, and $\Delta H_{a(c)}$ is equal to 64.2 kJ mol^{-1} (Boyd et al., 2015).

The Michaelis-Menten coefficient of RuBisCO's oxygenation acitivity, K_o (Pa) responds to temperature as well.

$$K_o = K_{o(25)} \exp\left[\Delta H_{a(o)} \frac{T - 298.15}{298.15RT}\right] \tag{16}$$

Where $K_{o(25)}$ is equal to 29.2 kPa, and $\Delta H_{a(o)}$ is equal to 10.5 kJ mol^{-1} (Boyd et al., 2015).

C_{bs} can be estimated as a function of mesophyll processes because the bundle-sheath is a semi-closed system and dependent on the mesophyll for the supply of CO_2 in the form of C_4 carboxylic acids. Thus, we can express C_{bs} mathematically as:

$$C_{bs} = L + (g_{bs} * C_m) \tag{17}$$

where C_{bs} and C_m are CO_2 concentrations in μ mol m^{-2}, g_{bs} is a constant 3 mmol m^{-2} s^{-1} (Von Caemmerer, 2000), and L is leakage in μ mol m^{-2} s^{-1}. We defined leakage as a fraction of photosynthetic assimilation:

$$L = l * A_L \tag{18}$$

where l was assumed to be non-varying, and we adopted a value of 0.01. We used equation 5 to calculate the value for A_L.

For direct comparison to trends seen in χ_m, we calculated the ratio of bundle sheath to atmospheric CO_2 as:

$$\chi_{bs} = C_{bs}/C_a \tag{19}$$

We solved for optimal V_{cmax} substituting the A_L from 5 for A_C in 14, yielding:

$$V_{cmax} = \frac{\phi I m \omega^*}{8\theta} \frac{C_{bs} + K_c(1 + O_{bs}/K_o)}{C_{bs} - \Gamma^*} \tag{20}$$

The optimal maximum rate of electron transport (J_{max}; μ mol m^{-2}s^{-1}) is calculated as in Smith et al. (Smith et al., 2019) as:

$$J_{max} = \phi I \omega \tag{21}$$

2.3 Parameterization of the Model

The free parameters in the theoretical model were defined based on empirical data (Table 1). Where possible, these were defined using data from C_4 species.

2.4 C_3 Comparison

We compared simulated photosynthetic rates from the C_4 acclimation model to an analogous C_3 presented in Smith et al. (2019) as updated in (Smith & Keenan, 2020) (model code available at DOI: 10.5281/zenodo.3874938). Both models rely upon the coordination hypothesis; however, in the C_4 model, there are three possible limiting rates, while the C_3 model has only two (A_P is unique to the C_4 model). While some parameters, such as those for A_L, are identical between the two models, others differ, though they are present in analogous equations. See table 1 for a full list of parameters with their respective C_3 and C_4 values.

In addition to comparing absolute values of assimilation rates, we also determined the difference between the rates as a percent of the C_3 level (ΔA):

$$\Delta A = \frac{A_{C_4} - A_{C_3}}{A_{C_3}} * 100 \tag{22}$$

A_{C3} and A_{C4} are the simulated rates of photosynthesis via the C_3 and C_4 pathways respectively. We made these comparisons across multiple CO_2 (200-1000 ppm), temperature (1-40 °C), PAR (0-1000 μmol m-2 s-1), and VPD values (1-8 kPa). In all cases, non-varying conditions were kept constant at standard conditions (CO_2 = 400 ppm, temperature = 25 °C, PAR = 800 μmol m-2 s-1, and VPD = 1).

Table 1: Photosynthetic Parameters (at 25°C) used in the model. The C_3 values are those that were used in the analogous C_3 model (Smith et al., 2019)

Parameter	C_4 Value	Unit	Reference	Equation	C_3 value
Θ	0.85	unitless	G. Farquhar and Wong (1984)	7 & 8	0.85
c	0.053	unitless	Smith et al. (2019)	4	0.053
Γ^*_{25}	2.6	Pa	-	10	4.332
$\Delta H_{a(g)}$	37830	J mol^{-1}	Bernacchi et al. (2001)	10	37830
$K_{p(25)}$	60.5	μmol mol^{-1}	Boyd et al. (2015)	12	-
$\Delta H_{a(p)}$	27.2	kJ mol^{-1}	Boyd et al. (2015)	12	-
$K_{c(25)}$	121	Pa CO_2	Boyd et al. (2015)	15	41.03
$\Delta H_{a(c)}$	64.2	kJ mol^{-1}	Boyd et al. (2015)	15	79.43
$K_{o(25)}$	29.2	kPa CO_2	Boyd et al. (2015)	16	28.21
$\Delta H_{a(o)}$	10.5	kJ mol^{-1}	Boyd et al. (2015)	16	36.38
g_{bs}	3	mmol m^{-1} s^{-1}	Von Caemmerer (2000)	17	-
l	0.01	unitless	-	18	-

2.5 Model Comparison to Global Relative C_4 Abundance

To estimate how well our model predicted observed patterns of C_4 species abundance, we predicted ΔA values globally and compared these values to relative abundance data from the International Satellite Land-Surface Climatology Project (Still et al., 2009). The data set estimates the percentage of vegetation (0-100) with the C_4 photosynthetic pathway. The data set is global, divided into 1° grid cells. For the comparison, we selected cells that fell within grasslands, open shrublands, savannas, and woody savannas, as defined by the MODIS Land Cover Type Product MCD12Q1 International Geosphere-Biosphere Programme (IGBP) legend and class descriptions (M. Friedl, 2015). These land cover types were selected because they each had high values of C_4 dominance. We fit a linear regression with ΔA as the dependent variable and the percentage of C_4 vegetation as the independent variable. We calculated Pearson's correlation coefficient to assess the strength of the relationship between our predicted ΔA value and the C_4 percent coverage.

2.6 Instantaneous Model

To compare the acclimated response to the unacclimated instantaneous response, we developed a second model without acclimation. This instantaneous model used the same parameters and core equations, but with static values for χ_m, χ_{bs}, J_{max}, V_{pmax}, and V_{cmax}. The values used were those predicted from the acclimated model under standard conditions (temperature = 25 °C, CO_2 = 400 ppm, PAR = 800 μ mol m^{-2} s^{-1}, elevation = 0 m ASL, and VPD = 1 kPa). We compared acclimated and unacclimated photosynthetic rates across a range of CO_2 (200-1000 ppm), temperature (1-40 °C), PAR (0-1000 μ mol m-2 s-1), and VPD_0 values (0-8 kPa). In all cases, non-varying conditions were kept constant at the standard conditions listed above.

3 Results

3.1 Optimal photosynthesis-environment responses

In response to increased temperature, our theory predicted an increase in χ_m (Figure 2). Two factors contributed to the increase: an increase in the Michaelis Menten con-

stant of PEPc (K_p) and a decrease in the viscosity of water (Equation 2). Increased VPD resulted in a non-linear decrease in χ_m directly due to D's presence in equation 2. Changes in CO_2 and PAR did not impact χ_m, as these conditions are not part of the theoretical equation (Equation 2).

The χ_{bs} value is coupled to mesophyll activities, as seen in equation 18. Therefore, χ_{bs} values do not follow the same patterns as χ_m (Figure 2). Not reflected in the scaled values in Figure 2, χ_{bs} has much higher absolute values (approx. 600% percent higher at standard conditions) under all conditions due to the carbon concentrating mechanism. In response to increased temperature, χ_{bs} increased non-linearly and eventually decreased at high temperatures. χ_{bs} increased linearly with PAR, in contrast to the lack of response to χ_m. This is seen because of the linear dependence of A_L on PAR as seen in equation 5 effects χ_{bs} in equation 18. χ_{bs} decreases non-linearly with CO_2 as C_m is increasing and A_L is unchanged. χ_{bs} decreases non-linearly with increasing VPD, driven by the decrease in C_m with VPD (Equations 1 & 2).

Predicted optimal J_{max} increases with temperature, PAR, and CO_2, and decreases slightly with VPD (Figure 3). The non-linear increase with temperature is due to the simultaneous increase of ϕ and Γ^* (within the ω term), which control J_{max} values linearly in equation 21. The linear increase with PAR is predicted in equation 21. Unlike the other biochemical processes, J_{max} increases very slightly with CO_2. Finally, J_{max} decreases with VPD due to decreases in C_m within the ω term (Equations6 and 8).

The model predicts an increase in V_{pmax} with temperature and PAR (Figure 3). As noted in equation 12, the Michaelis-Menten constant, K_p is temperature dependent, as is ϕ (Equation 9). As both are present in the numerator of equation 13, V_{pmax} increases with temperature. V_{pmax} increased linearly in response to PAR, as a result of a linear increase in A_L. V_{pmax} decreased in response to increasing CO_2 levels, as more CO_2 allowed for downregulation of PEP carboxylation necessary to equate A_L and A_p. The model predicted a slight, non-linear, increase in V_{pmax} with increased vapor pressure deficit due to reduced χ_m.

Like V_{pmax}, the optimal V_{cmax} increases with temperature and PAR and decreases with CO_2 due to similar drivers (Figure 3). The temperature increases continuously within the physiologically relevant range, rather than peaking before 40 °C due to the combined effects increases in K_c and Γ^* (Equation 20). V_{cmax} increases with PAR non-linearly. The non-linear relationship is due to the dependence of χ_{bs} on PAR (Equation 17) in addition to the linear relationship of A_L with PAR (Equation 20). The decrease of V_{cmax} in response to increased CO_2 is due to a down-regulation of carboxylation activity to match A_C rates to the unaffected A_L rates. V_{cmax} decreases to a lesser degree than V_{pmax} with increasing CO_2 due to the greater partial pressure of CO_2 in the bundle sheath as compared to the mesophyll. V_{cmax} decreased very slightly in response to VPD, due to a decrease in O_{bs} while χ_{bs} remains relatively constant. From a VPD of 0 to 8, O_{bs} drops by 69%, while χ_{bs} drops by only 42%. Lower O_{bs} values result in a decrease of RuBisCO's oxygenase activity, allowing RuBisCO to achieve the same carboxylation rates at lower V_{cmax} values. A decrease in V_{cmax} is predicted in Equation 20 because O_{bs} in the numerator, so a lower O_{bs} value will lead to a lower V_{cmax} value.

3.2 Allocation of Resources to Different Biochemical Processes

Figure 4 shows the ratios of J_{max} to V_{cmax}, J_{max} to V_{pmax}, and V_{cmax} to V_{pmax} across varying temperature and PAR values. J_{max}:V_{cmax} decreases with temperature, as the increase of the V_{cmax} with temperature quickly outpaces the increase of J_{max}. The J_{max}:V_{cmax} ratio increases with PAR as J_{max} increases linearly. The ratio of J_{max} to V_{pmax} remains relatively constant across both the temperature and the PAR gradients. J_{max}:V_{pmax} decreased by only 16% across the temperature range, and does not change across the PAR gradient. This muted response is due to J_{max} and V_{pmax}'s similar responses as seen in figure 3. The V_{cmax} to V_{pmax} ratio increases with temperature and decreases with PAR. The increase of V_{cmax}:V_{pmax} with temperature is due to V_{cmax}'s large absolute values

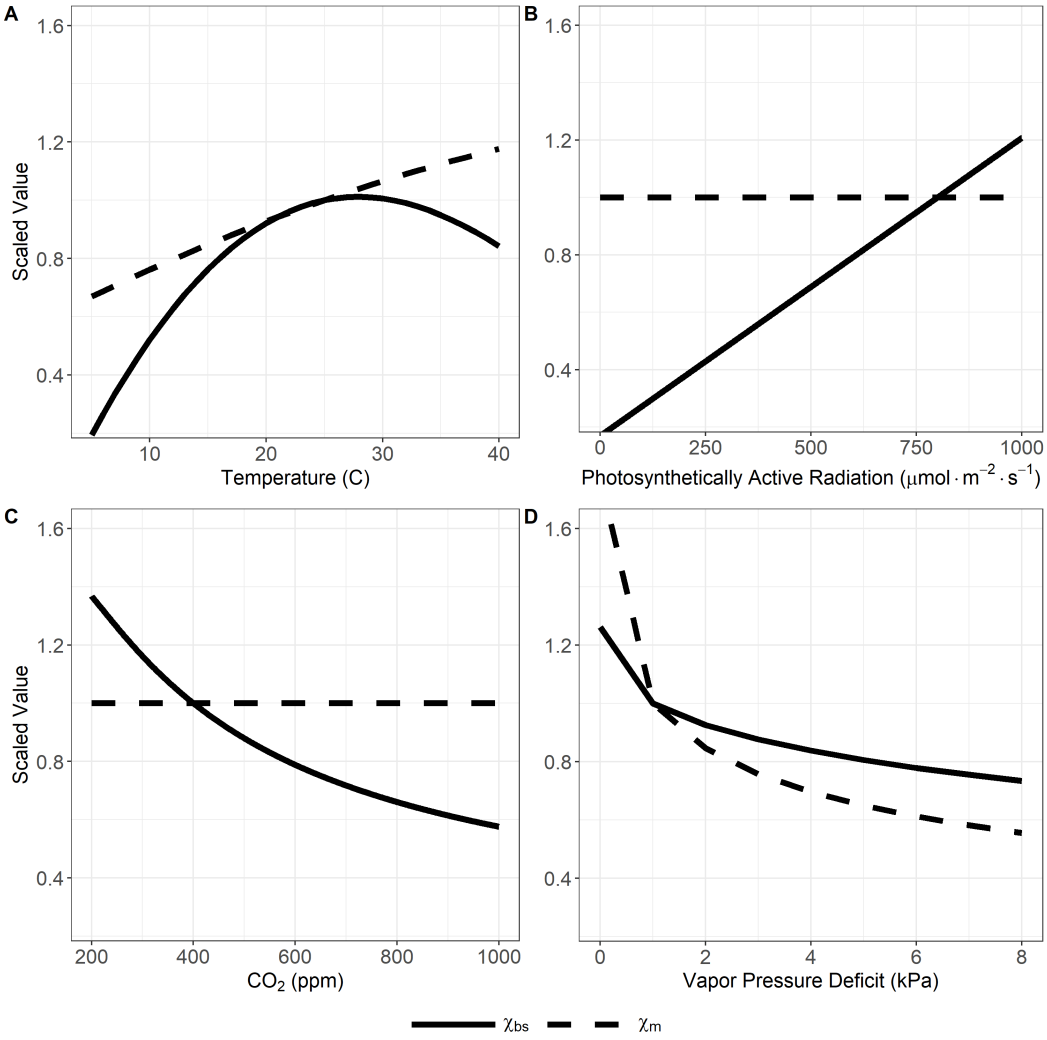

Figure 2: Response of χ_m (dashed black line) and χ_{bs} (solid black line) to (A) temperature, (B) PAR, (C) atmospheric CO_2, and (D) vapor pressure when all others are held constant at standard values. Values are standardized to the predicted value at "standard" conditions (temperature = 25 °C, CO_2 = 400 ppm, PAR = 800 μ mol m^{-2} s^{-1} PAR, elevation = 0 m ASL, and VPD = 1 kPa).

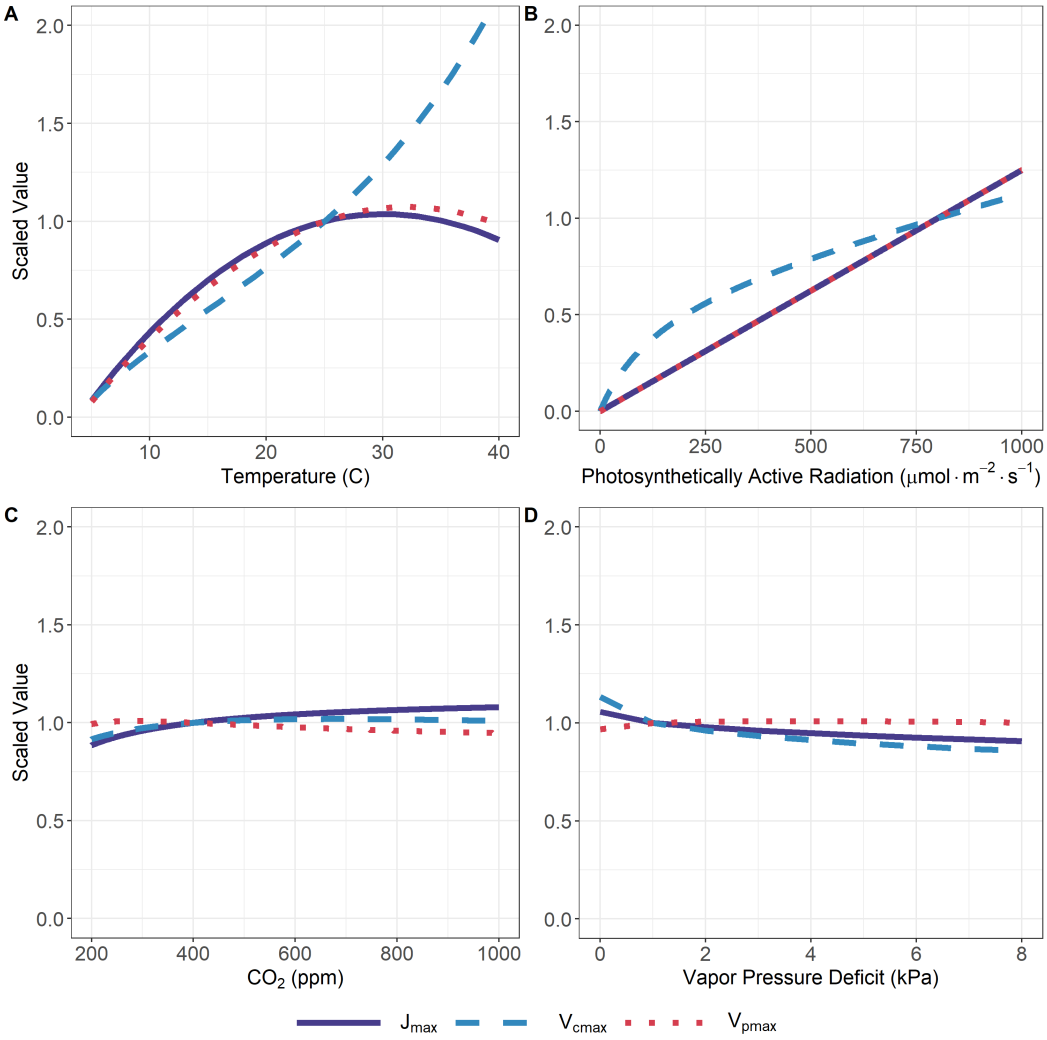

Figure 3: Response of optimal J_{max} (solid purple line), V_{cmax}(dashed blue line), and V_{pmax} (dotted red line) to (A) temperature, (B) PAR, (C) atmospheric CO_2, and (D) vapor pressure when all others are held constant at standard values. Values are standardized to the predicted value at "standard" conditions (temperature = 25 °C, CO_2 = 400 ppm, PAR = 800 μ mol m^{-2} s^{-1}, elevation = 0 m ASL, and VPD = 1 kPa).

due to the carbon concentrating mechanism, and V_{cmax}'s increase with temperature. None of the ratios changed significantly with CO_2 or VPD.

3.3 Predicted optimal photosynthetic rates

Predicted optimal A increased non-linearly with temperature to approximately 25°C after which it decreased (Figure 5). A increased linearly with PAR, concurrent with increases in biochemical process rates. A increases with atmospheric CO_2 and decreases with VPD.
C_4 photosynthetic rates simulated by this model were higher than the C_3 rates predicted by the Smith et al. (2019) model under all environmental conditions (Figure 5). Photosynthetic rates were most similar at low light, low temperature, and high CO_2 levels.

3.4 Acclimated Versus Non-Acclimated Responses

Optimal photosynthetic acclimation either increased assimilation or decreased photosynthetic costs (Figure 5). For all environmental conditions, when the environmental variables are equal to the acclimated conditions, assimilation rates in the acclimated and instantaneous models are equal. For temperatures above or below the acclimation temperature, the assimilation was higher for the acclimated model. With increasing PAR, instantaneous assimilation is unable to increase beyond the acclimated condition, and plateaus, whereas the acclimation model continues to increase linearly. Similarly, with increasing CO_2 the rate of increase of assimilation slows above the acclimated value of CO_2. However, acclimation results in decreased assimilation with increasing VPDs. The instantaneous model is unresponsive to VPD because χ_m is not decreasing. While the open stomata do lead to higher assimilation, remaining open would result water loss that the acclimated plant avoids by decreasing assimilation.

3.5 Model-Data Comparison

Global values for ΔA correlated strongly with the percent of vegetation with the C_4 photosynthetic pathway from the International Satellite Land-Surface Climatology Project (Still et al., 2009) (P ¡ 0.001; Figure 6). This indicates that our model captures trends in the distribution of plants with different photosynthetic types globally.

4 Discussion

The C_4 photosynthetic pathway accounts for 20% of global carbon assimilation and is present in many critical agricultural species, including maize (Ehleringer et al., 1997). While C_4 species are known to acclimate to changes in environmental conditions (R. F. Sage & McKown, 2006), ESMs do not include this acclimation. Here, we present a novel theoretical model for C_4 photosynthetic acclimation suitable for use in ESMs. In addition to its potential to improve ESM simulations' reliability, the theoretical model may also be informative for understanding other ecological aspects of C_4 species, including their competition with C_3 species under different environmental contexts. Below we discuss the insights we gleaned from this model exercise and its potential for improving our understanding of plant ecology under variable environments.

4.1 Insights into Photosynthetic Efficiency and Plasticity

Our theory provides insights into long appreciated aspects of C_4 photosynthesis, including the mechanisms underlying their water and nutrient use efficiencies and photosynthetic plasticity. First, our theory's broad fidelity to global observation-based estimates of C_4 species abundance suggests that, across large spatial scales, realized assimilation

is principally determined by the optimization in response to environmental conditions. It is essential to note that photosynthetic data for C_4 plants is more scarce than data available for C_3 plants (Kattge & Sandel, 2020), limiting our ability to more directly test the model's mechanisms. Nonetheless, our theory provides a framework for developing hypotheses for how C_4 photosynthesis varies across environments. It will be critical to explore these responses across a range of temporal scales as more data becomes available.

Second, equation 2 predicts χ_m to be 0.56 under "standard" conditions (temperature = 25 °C, CO_2 = 400 ppm, PAR = 800 μ mol m^{-2} s^{-1}, elevation = 0 m ASL, and VPD = 1 kPa). This χ value is considerably lower than values found in C_3 plants (Wang et al., 2017), indicating higher WUE in C_4 plants than C_3 plants. Our theory confirms that this observed difference between photosynthetic types is due to the relative lack of oxygenation in C_4 plants (R. F. Sage, 1999; R. F. Sage & McKown, 2006).

Third, the increased concentrations of CO_2 at the site of RuBisCO fixation (C_{bs}) relative to that in C_3 plants allows for a reduced need for RuBisCO enzymes, thus leading to potentially greater NUE in C_4 plants. Greater NUE in C_4 versus C_3 has been observed previously (R. F. Sage & Pearcy, 1987). Our theory confirms previous estimates indicating that this is due to RuBisCO's greater efficiency due to reduced oxygenation and further reinforces the importance of high C_{bs} in driving this response (R. F. Sage et al., 1987).

Finally, our theory sheds light on the photosynthetic plasticity observed in C_4 plants. Experimental studies have shown that C_4 photosynthesis is less sensitive than C_3 photosynthesis in general (R. F. Sage & McKown, 2005) and in response to CO_2 (Ainsworth & Long, 2005) and VPD (Wherley & Sinclair, 2009) in particular. The CO_2 and VPD responses are consistent with our theory. Importantly, our theory confirms that this is due to greater efficiency afforded to C_4 species by concentrating a high amount of CO_2 in the bundle sheath. Notably, our theory also finds high plasticity in response to temperature and PAR, similar to that of C_3 species, suggesting that the mechanisms driving acclimation to these conditions (Wang et al., 2017; Smith et al., 2019; Smith & Keenan, 2020) are similar across species with different photosynthetic types, confirming previous experimental results in response to temperature (Yamori et al., 2014; Smith & Dukes, 2017). However, previous experimental results suggest the PAR response of C_4 species to be less plastic than C_3 species (R. F. Sage & McKown, 2005), contrasting with our results. Coupled theory-experiment analyses would help to understand further the mechanisms driving this disconnect.

4.2 Acclimation to elevated temperature and CO_2 reduces optimal enzyme requirements, possibly reducing nitrogen use

These results suggest that future, warmer conditions may increase simulated photosynthesis of C_4 plants (Figure 5). However, our theory suggests that this will come alongside a reduction in nitrogen-heavy carboxylation enzymes, possibly increasing future nutrient-use efficiency (NUE), as has been suggested for C_3 plants (Smith & Keenan, 2020).

The potential reduction in leaf-level nitrogen demand suggested by our theory may critically impact ESM simulations that include a dynamic N cycle. Such models indicate that progressive nitrogen limitation will limit increases in future productivity driven by increases in atmospheric CO_2 (Wieder et al., 2015; Thornton et al., 2007b; P. Reich et al., 2006; Zhu et al., 2019; Finzi et al., 2007; Luo et al., 2004). To correctly predict the magnitude and extent of progressive nitrogen limitation, models of photosynthesis must correctly simulate changing leaf NUE. Our theory predicts increased NUE in the future, driven by a critical tenant of the least-cost hypothesis: maximizing photosynthesis while minimizing nutrient use (Wright et al., 2003). Acclimation led to increased NUE in C_3 plants in models (Smith & Keenan, 2020), and in the field (Davey et al., 1999). Long-term field experiments with C_4 plants observed increased NUE in response to warming and elevated CO_2 (Carvalho et al., 2020). These results suggest that future increases in

leaf NUE must be considered by ESMs to predict future ecosystem N limitation accurately. Our model provides an avenue for doing this for C_4 plants.

4.3 C_4 advantage will decrease in future

Our theory indicates that future high temperature, high CO_2 environments will disproportionately favor C_3 plants over C_4 plants. While we expected C_3 photosynthetic rates to increase with temperature and CO_2 (Smith & Dukes, 2013), we expected C_4 plants to increase with temperature only (Alberto et al., 1996), while remaining unchanged or to increase very little in response to CO_2 (R. Sage & Coleman, 2001; Poorter & Navas, 2003). Our model predicted these results when compared to the analogous C_3 model (Smith et al., 2019). We found that the ΔA value increased with temperature and decreased with CO_2. When the two vary simultaneously, C_4 retain their current competitive advantage in high CO_2 environments only when the acclimated temperature is also very high. For example, at a growing season temperature of 15°C at 400 ppm CO_2, C_4 photosynthesis assimilates roughly 26% more carbon than C_3 photosynthesis. However, this same ΔA value can only be achieved at a growing season temperature of 37 °C when CO_2 reaches 1000 ppm. Looking forward, these comparisons may indicate future restrictions of C_4 species to extremely hot environments. A similar comparison between ΔA values at current (400 ppm) and low (250 ppm) CO_2 values can also be used to infer evolutionary history of C_4 plants, many of which first appeared when CO_2 levels were much lower than they are today.

Previous results question the longevity of such a competitive decline of C_4 plants when plants acclimate to increased CO_2 levels on a multi-decadal timescale (P. B. Reich et al., 2018). That study and others (Wolf & Ziska, 2018) indicate the importance of including nutrient feedbacks, plant growth rates, and plant life spans in systems where nutrients or water may be limiting. The ability of C_4 plants to accumulate organic matter in the soil may further help C_4 plants to thrive in nutrient and water poor environments, and may help to ameliorate the ΔA differential caused by high CO_2 concentrations, keeping C_4 plants competitive in a greater number of habitats. Coupling our theory to a model that can predict these higher-order processes is the next step in understanding the interplay between leaf photosynthesis and ecosystem-scale processes.

Acknowledgments

All data, model code, and analysis code, including code to reproduce the figures have been published in an open-access repository (DOI: 10.5281/zenodo.4420326)

References

Ainsworth, E. A., & Long, S. P. (2005). What have we learned from 15 years of free-air co2 enrichment (face)? a meta-analytic review of the responses of photosynthesis, canopy properties and plant production to rising co2. *New Phytologist*, *165*(2), 351-372.

Alberto, A., Ziska, L., Cervancia, C., & Manalo, P. (1996, 01). The influence of increasing carbon dioxide and temperature on competitive interactions between a c3 crop, rice (oryza sativa) and a c4 weed (echinochloa glabrescens). *Functional Plant Biology*, *23*, 795-802.

Bazzaz, F. A. (1990). The response of natural ecosystems to the rising global co2 levels. *Annual review of ecology and systematics*, *21*(1), 167–196.

Bellasio, C., & Griffiths, H. (2014). Acclimation to low light by c4 maize: implications for bundle sheath leakiness. *Plant, cell & environment*, *37*(5), 1046–1058.

Bernacchi, C., Pimentel, C., & Long, S. (2003). In vivo temperature response functions of parameters required to model rubp-limited photosynthesis. *Plant, Cell*

& Environment, *26*(9), 1419–1430.

Bernacchi, C., Singsaas, E., Pimentel, C., Portis Jr, A., & Long, S. (2001). Improved temperature response functions for models of rubisco-limited photosynthesis. *Plant, Cell & Environment*, *24*(2), 253–259.

Berry, J., & Bjorkman, O. (1980). Photosynthetic response and adaptation to temperature in higher plants. *Annual Review of plant physiology*, *31*(1), 491–543.

Boardman, N. t. (1977). Comparative photosynthesis of sun and shade plants. *Annual review of plant physiology*, *28*(1), 355–377.

Booth, B. B., Jones, C. D., Collins, M., Totterdell, I. J., Cox, P. M., Sitch, S., ... Lloyd, J. (2012). High sensitivity of future global warming to land carbon cycle processes. *Environmental Research Letters*, *7*(2), 024002.

Boyd, R. A., Gandin, A., & Cousins, A. B. (2015). Temperature responses of c4 photosynthesis: biochemical analysis of rubisco, phosphoenolpyruvate carboxylase, and carbonic anhydrase in setaria viridis. *Plant Physiology*, *169*(3), 1850–1861.

Carvalho, J., Ferreira Barreto, R., Prado, R., Habermann, E., Branco, R., & Martinez, C. (2020, 03). Elevated co2 and warming change the nutrient status and use efficiency of panicum maximum jacq. *PLOS ONE*, *15*, e0223937.

Chen, J.-L., Reynolds, J. F., Harley, P. C., & Tenhunen, J. D. (1993). Coordination theory of leaf nitrogen distribution in a canopy. *Oecologia*, *93*(1), 63–69.

Collatz, G. J., Ball, J. T., Grivet, C., & Berry, J. A. (1991). Physiological and environmental regulation of stomatal conductance, photosynthesis and transpiration: a model that includes a laminar boundary layer. *Agricultural and Forest meteorology*, *54*(2-4), 107–136.

Collatz, G. J., Ribas-Carbo, M., & Berry, J. (1992). Coupled photosynthesis-stomatal conductance model for leaves of c4 plants. *Functional Plant Biology*, *19*(5), 519–538.

Cornwell, W. K., Wright, I. J., Turner, J., Maire, V., Barbour, M. M., Cernusak, L. A., ... others (2018). Climate and soils together regulate photosynthetic carbon isotope discrimination within c3 plants worldwide. *Global ecology and biogeography*, *27*(9), 1056–1067.

Davey, P., Parsons, A., Atkinson, L., Wadge, K., & Long, S. P. (1999). Does photosynthetic acclimation to elevated co2 increase photosynthetic nitrogen-use efficiency? a study of three native uk grassland species in open-top chambers. *Functional Ecology*, *13*, 21–28.

Dusenge, M. E., Duarte, A. G., & Way, D. A. (2019). Plant carbon metabolism and climate change: elevated co 2 and temperature impacts on photosynthesis, photorespiration and respiration. *New Phytologist*, *221*(1), 32–49.

Dwyer, S. A., Ghannoum, O., Nicotra, A., & Von Caemmerer, S. (2007). High temperature acclimation of c4 photosynthesis is linked to changes in photosynthetic biochemistry. *Plant, Cell & Environment*, *30*(1), 53–66.

Ehleringer, J., Cerling, T., & Helliker, B. (1997, 10). C-4 photosynthesis, atmospheric co2 and climate. *Oecologia*, *112*, 285-299.

Farquhar, G., & Wong, S. (1984). An empirical model of stomatal conductance. *Functional Plant Biology*, *11*(3), 191–210.

Farquhar, G. D., von Caemmerer, S. v., & Berry, J. A. (1980). A biochemical model of photosynthetic co 2 assimilation in leaves of c 3 species. *planta*, *149*(1), 78–90.

Finzi, A. C., Norby, R. J., Calfapietra, C., Gallet-Budynek, A., Gielen, B., Holmes, W. E., ... others (2007). Increases in nitrogen uptake rather than nitrogen-use efficiency support higher rates of temperate forest productivity under elevated co2. *Proceedings of the National Academy of Sciences*, *104*(35), 14014–14019.

Friend, A. D. (2010). Terrestrial plant production and climate change. *Journal of experimental botany*, *61*(5), 1293–1309.

Kanai, R., & Edwards, G. E. (1999). The biochemistry of c4 photosynthesis. *C4 plant biology*, *49*, 87.

Kattge, J., & Knorr, W. (2007). Temperature acclimation in a biochemical model of photosynthesis: a reanalysis of data from 36 species. *Plant, cell & environment*, *30*(9), 1176–1190.

Kattge, J., & Sandel, B. (2020). Try plant trait database-enhanced coverage and open access (vol 2020, pg 119, 2020). *Global Change Biology*, *26*(9), 5343–5343.

King, A. W., Gunderson, C. A., Post, W. M., Weston, D. J., & Wullschleger, S. D. (2006). Plant respiration in a warmer world. *Science*, *312*(5773), 536–537.

Krall, J., Edwards, G., & Ku, M. (1991). Quantum yield of photosystem ii and efficiency of co2 fixation in flaveria (asteraceae) species under varying light and co2. *Functional Plant Biology*, *18*(4), 369–383.

Lombardozzi, D. L., Bonan, G. B., Smith, N. G., Dukes, J. S., & Fisher, R. A. (2015). Temperature acclimation of photosynthesis and respiration: A key uncertainty in the carbon cycle-climate feedback. *Geophysical Research Letters*, *42*(20), 8624–8631.

Luo, Y., Su, B., Currie, W. S., Dukes, J. S., Finzi, A., Hartwig, U., ... others (2004). Progressive nitrogen limitation of ecosystem responses to rising atmospheric carbon dioxide. *Bioscience*, *54*(8), 731–739.

Maherali, H., Reid, C., Polley, H., Johnson, H., & Jackson, R. (2002). Stomatal acclimation over a subambient to elevated co2 gradient in a c3/c4 grassland. *Plant, Cell & Environment*, *25*(4), 557–566.

Maire, V., Martre, P., Kattge, J., Gastal, F., Esser, G., Fontaine, S., & Soussana, J.-F. (2012). The coordination of leaf photosynthesis links c and n fluxes in c3 plant species. *PloS one*, *7*(6), e38345.

Mercado, L. M., Medlyn, B. E., Huntingford, C., Oliver, R. J., Clark, D. B., Sitch, S., ... Cox, P. M. (2018). Large sensitivity in land carbon storage due to geographical and temporal variation in the thermal response of photosynthetic capacity. *New Phytologist*, *218*(4), 1462–1477.

M. Friedl, D. S.-M. (2015). *Mcd12q1 modis/terra+aqua land cover type yearly l3 global 500m sin grid v006.* NASA EOSDIS Land Processes DAAC. Retrieved from `https://lpdaac.usgs.gov/products/mcd12q1v006/` doi: 10.5067/MODIS/MCD12Q1.006

Oberhuber, W., & Edwards, G. E. (1993). Temperature dependence of the linkage of quantum yield of photosystem ii to co2 fixation in c4 and c3 plants. *Plant Physiology*, *101*(2), 507–512.

Poorter, H., & Navas, M.-L. (2003, 02). Plant growth and competition at elevated co2: on winners, losers and functional groups: Tansley review. *New Phytologist*, *157*, 175 - 198.

Prentice, I. C., Dong, N., Gleason, S. M., Maire, V., & Wright, I. J. (2014). Balancing the costs of carbon gain and water transport: testing a new theoretical framework for plant functional ecology. *Ecology Letters*, *17*(1), 82–91.

Reich, P., Hobbie, S., Lee, T., Ellsworth, D., West, J., Tilman, D., ... Trost, J. (2006, 05). Nitrogen limitation constrains sustainability of ecosystem response to co2. *Nature*, *440*, 922-5.

Reich, P. B., Hobbie, S. E., Lee, T. D., & Pastore, M. A. (2018). Unexpected reversal of c3 versus c4 grass response to elevated co2 during a 20-year field experiment. *Science*, *360*(6386), 317–320.

Sage, R., & Coleman, J. (2001, 01). Effects of low atmospheric co2 on plants: more than a thing of the past. *Trends Plant Sci*, *6*, 1360-1385.

Sage, R., & Kubien, D. (2007). The temperature response of c3 and c4 photosynthesis. *Plant, cell & environment*, *30*(9), 1086–1106.

Sage, R. F. (1999). Why c4 photosynthesis. *C4 plant biology*, 3–16.

Sage, R. F., & McKown, A. D. (2005, 12). Is C4 photosynthesis less phenotypically

plastic than C3 photosynthesis?*. *Journal of Experimental Botany*, *57*(2), 303-317.

Sage, R. F., & McKown, A. D. (2006). Is c4 photosynthesis less phenotypically plastic than c3 photosynthesis? *Journal of experimental botany*, *57*(2), 303–317.

Sage, R. F., & Pearcy, R. W. (1987). The nitrogen use efficiency of c3 and c4 plants. *Plant Physiology*, *84*(3), 959–963.

Sage, R. F., Pearcy, R. W., & Seemann, J. R. (1987). The nitrogen use efficiency of c3 and c4 plants. *Plant Physiology*, *85*(2), 355–359.

Smith, N. G., & Dukes, J. S. (2013). Plant respiration and photosynthesis in global-scale models: incorporating acclimation to temperature and co2. *Global Change Biology*, *19*(1), 45–63.

Smith, N. G., & Dukes, J. S. (2017). Short-term acclimation to warmer temperatures accelerates leaf carbon exchange processes across plant types. *Global change biology*, *23*(11), 4840–4853.

Smith, N. G., & Keenan, T. F. (2020). Mechanisms underlying leaf photosynthetic acclimation to warming and elevated co2 as inferred from least-cost optimality theory. *Global Change Biology*.

Smith, N. G., Keenan, T. F., Colin Prentice, I., Wang, H., Wright, I. J., Niinemets, Ü., ... others (2019). Global photosynthetic capacity is optimized to the environment. *Ecology letters*.

Smith, N. G., Lombardozzi, D., Tawfik, A., Bonan, G., & Dukes, J. S. (2017). Biophysical consequences of photosynthetic temperature acclimation for climate. *Journal of Advances in Modeling Earth Systems*, *9*(1), 536–547.

Smith, N. G., Malyshev, S. L., Shevliakova, E., Kattge, J., & Dukes, J. S. (2016). Foliar temperature acclimation reduces simulated carbon sensitivity to climate. *Nature Climate Change*, *6*(4), 407–411.

Still, C. J., Berry, J. A., Collatz, G. J., & DeFries, R. S. (2009). Islscp initiative ii collection. data set.

Thornton, P., Lamarque, J., Rosenbloom, N., & Mahowald, N. (2007a). Effects of terrestrial carbon-nitrogen cycle coupling on climate-carbon cycle dynamics. *Global Biogeochemical Cycles*, *21*.

Thornton, P., Lamarque, J.-F., Rosenbloom, N., & Mahowald, N. (2007b, 12). Influence of carbon-nitrogen cycle coupling on land model response to co2 fertilization and climate variability. *Global Biogeochemical Cycles*, *21*.

Von Caemmerer, S. (2000). *Biochemical models of leaf photosynthesis*. Csiro publishing.

Von Caemmerer, S., & Furbank, R. T. (1999). Modeling c4 photosynthesis. *C4 plant biology*, 173–211.

Wang, H., Prentice, I. C., Keenan, T. F., Davis, T. W., Wright, I. J., Cornwell, W. K., ... Peng, C. (2017). Towards a universal model for carbon dioxide uptake by plants. *Nature plants*, *3*(9), 734.

Way, D. A., & Yamori, W. (2014). Thermal acclimation of photosynthesis: on the importance of adjusting our definitions and accounting for thermal acclimation of respiration. *Photosynthesis research*, *119*(1-2), 89–100.

Wherley, B. G., & Sinclair, T. R. (2009). Differential sensitivity of c3 and c4 turfgrass species to increasing atmospheric vapor pressure deficit. *Environmental and Experimental Botany*, *67*(2), 372 - 376.

Wieder, W., Cleveland, C., Smith, W., & Todd-Brown, K. (2015, 04). Future productivity and carbon storage limited by terrestrial nutrient availability. *Nature Geoscience*, *8*, 441-444.

Wolf, J., & Ziska, L. (2018). Comment on "unexpected reversal of c3 versus c4 grass response to elevated co2 during a 20-year field experiment". *Science*, *361*(6402).

Wright, I., Reich, P., & Westoby, M. (2003, 02). Least-cost input mixtures of water and nitrogen for photosynthesis. *The American naturalist*, *161*, 98-111.

Yamori, W., Hikosaka, K., & Way, D. A. (2014). Temperature response of photosynthesis in c 3, c 4, and cam plants: temperature acclimation and temperature adaptation. *Photosynthesis research*, *119*(1-2), 101–117.

Zaehle, S., & Friend, A. (2010). Carbon and nitrogen cycle dynamics in the o-cn land surface model: 1. model description, site-scale evaluation, and sensitivity to parameter estimates. *Global Biogeochemical Cycles*, *24*(1).

Zhou, H., Helliker, B. R., Huber, M., Dicks, A., & Akçay, E. (2018). C4 photosynthesis and climate through the lens of optimality. *Proceedings of the National Academy of Sciences*, *115*(47), 12057–12062.

Zhu, Q., Riley, W. J., Tang, J., Collier, N., Hoffman, F. M., Yang, X., & Bisht, G. (2019). Representing nitrogen, phosphorus, and carbon interactions in the e3sm land model: Development and global benchmarking. *Journal of Advances in Modeling Earth Systems*, *11*(7), 2238–2258.

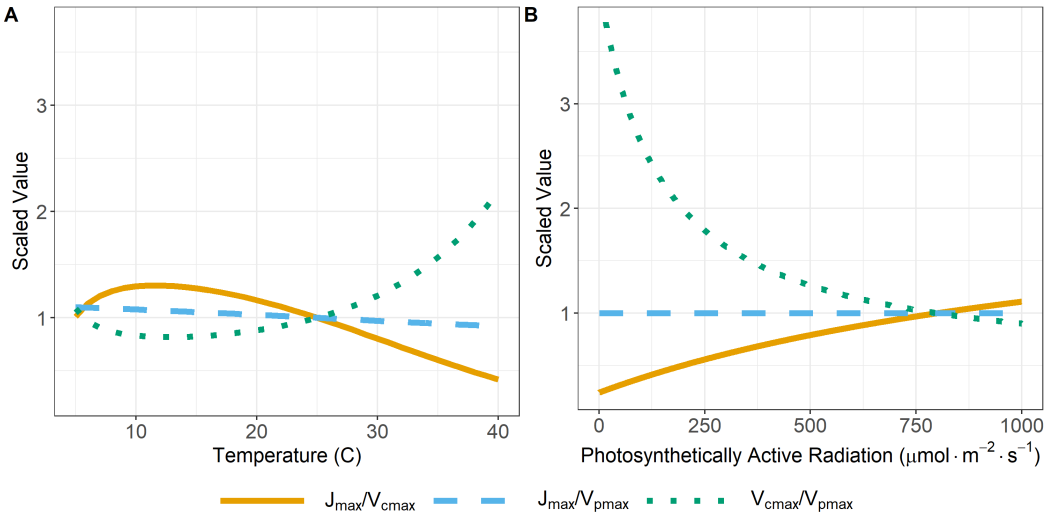

Figure 4: Predicted response of optimal ratios of J_{max}:V_{cmax} (solid yellow line), J_{max}:V_{pmax} (dashed blue line), and V_{cmax}:V_{pmax} (dotted green line) to (A) temperature and (B) PAR when all other conditions are held constant at standard values. Values are standardized to the predicted value at "standard" conditions (temperature = 25 °C, CO_2 = 400 ppm, PAR = 800 μ mol m^{-2} s^{-1}, elevation = 0 m ASL, and VPD = 1 kPa).

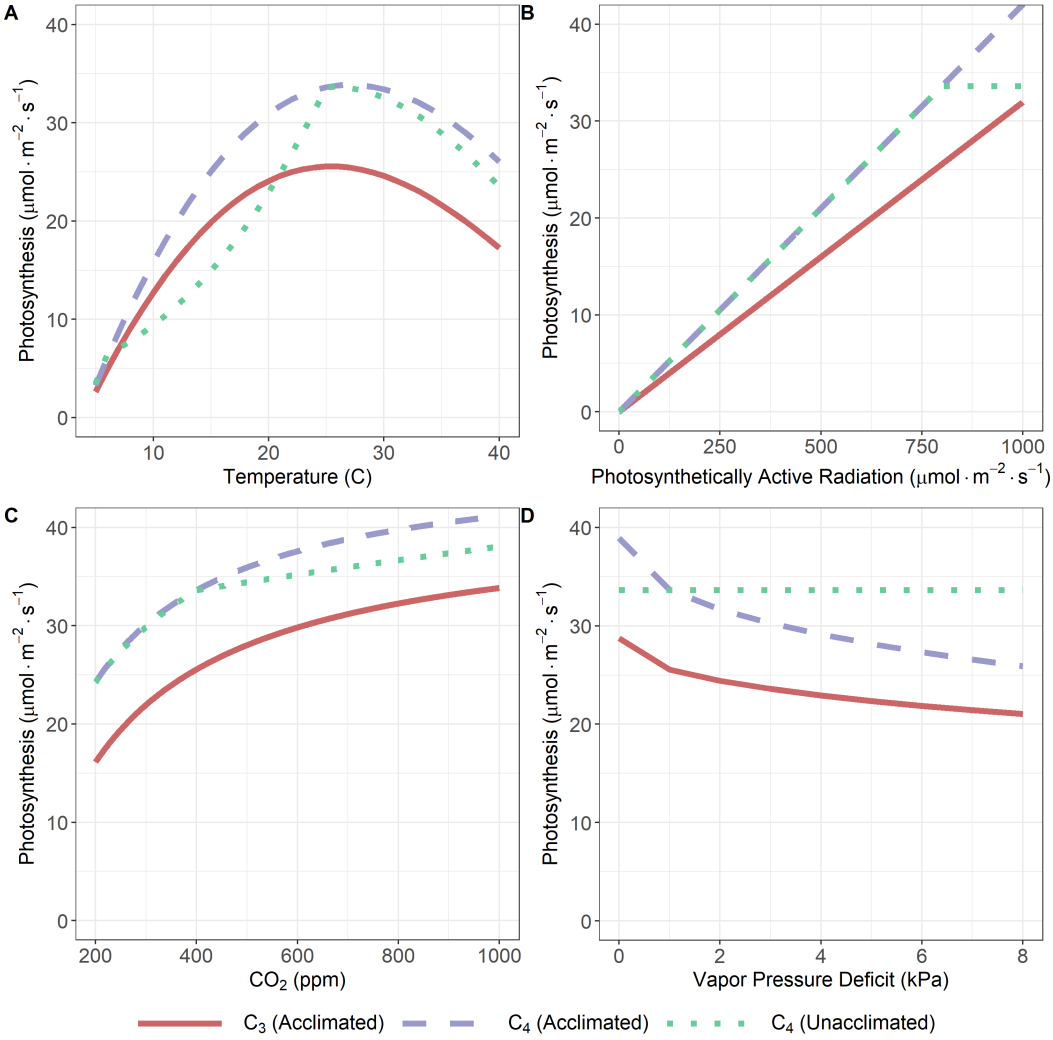

Figure 5: Predicted photosynthetic assimilation by acclimated C_4 plants (dashed purple line), unacclimated C_4 plants (dotted green line) and acclimated C_3 plants (solid red line) varies with (A) temperature, (B) PAR, (C) atmospheric CO_2, and (D) vapor pressure deficit when all other conditions are held constant at standard values (temperature = 25 °C, CO_2 = 400 ppm, PAR = 800 μ mol m^{-2} s^{-1}, elevation = 0 m ASL, and VPD = 1 kPa). C_4 rates were predicted from the model presented in the text, while C_3 rates were predicted from(Smith et al., 2019) as updated in (Smith & Keenan, 2020) (DOI: 10.5281/zenodo.3874938). In both cases, similar ϕ values were used.

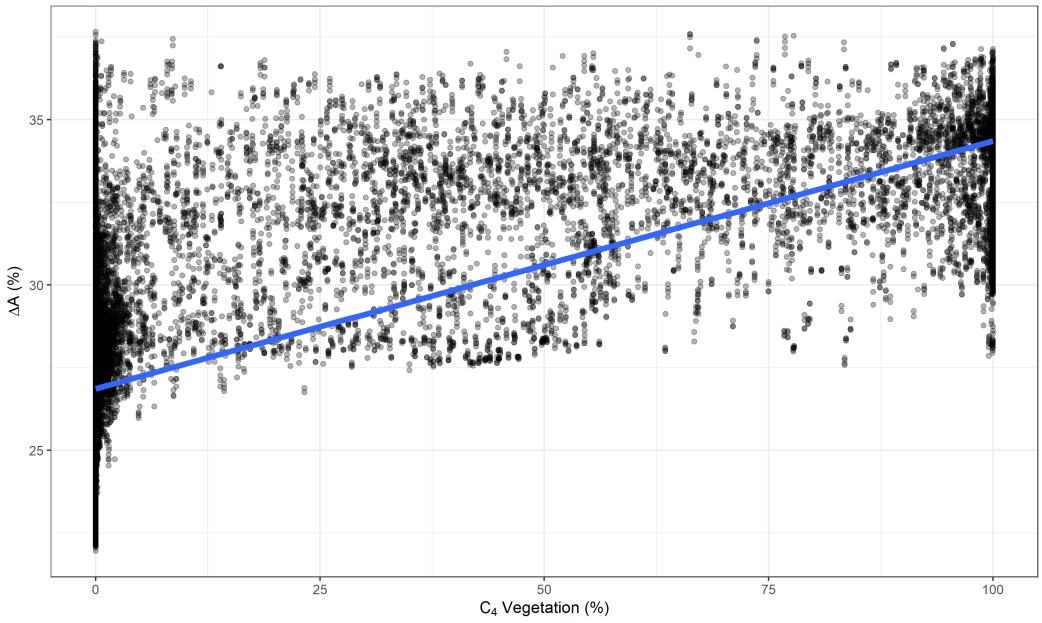

Figure 6: Relationship between the predicted optimal photosynthetic advantage of C_4 over C_3 plants (ΔA) to the percentage of C_4 vegetation from the International Satellite Land-Surface Climatology Project (Still et al., 2009). Points represent 1° gridcells in locations described by MODIS as grasslands, open shrublands, savannas, or woody savannas. Insert statistics show the statistics from a linear model relationship of ΔA and percent C_4 vegetation. The blue line show the fit from the linear model.